

# We are IntechOpen, the world's leading publisher of Open Access books Built by scientists, for scientists

5,000

Open access books available

124,000

International authors and editors

140M

Downloads

Our authors are among the

154

Countries delivered to

TOP 1%

most cited scientists

12.2%

Contributors from top 500 universities



WEB OF SCIENCE™

Selection of our books indexed in the Book Citation Index  
in Web of Science™ Core Collection (BKCI)

Interested in publishing with us?  
Contact [book.department@intechopen.com](mailto:book.department@intechopen.com)

Numbers displayed above are based on latest data collected.  
For more information visit [www.intechopen.com](http://www.intechopen.com)



# Ferrite Materials and Applications

*Tsun-Hsu Chang*

## Abstract

This chapter starts from a generalized permeability and aims at providing a better understanding of the ferrites behavior in the microwave fields. The formula of the generalized permeability explains why the permeability of the ferrimagnetic or even the ferromagnetic materials strongly depends on the applied magnetic bias and the polarization of the wave. Right-hand circularly polarized (RHCP) wave may synchronize with the precession of the magnetic moment, resulting in a strong resonant effect. Characterizing the ferrites' properties, including the complex permittivity, the saturation magnetization, and the resonance linewidth, will be discussed. We then utilize these properties to design and fabricate various microwave devices, such as phase shifters, circulators, and isolators. Detailed analysis and simulation to demonstrate how these ferrite devices work will be shown. The mechanism will be discussed.

**Keywords:** ferrite, microwave, generalized permeability, circular polarization, phase shifter, circulator, isolator

## 1. Introduction

Ferrimagnetism is similar to ferromagnetism in many ways [1–4]. They all have hysteresis curves as the applied magnetic field changes, resulting in the saturation magnetization ( $4\pi M_s$ ), the coercive field ( $H_c$ ), and the remnant polarization ( $B_r$ ). A ferri- or ferromagnetic material can be used to fabricate a hard or a soft magnet depending on its coercivity ( $H_c$ ). Hard magnets are characterized by a high  $H_c$ , indicating that their magnetization is difficult to change and will retain their magnetization in the absence of an applied field as shown in **Figure 1(a)**. On the contrary, the soft magnets have low  $H_c$  values and, normally, have very weak, remnant magnetic field (low  $B_r$ ) as in **Figure 1(b)**. Hard magnetism has been extensively used to make the permanent magnets and provides a strong DC magnetic field, while the soft magnetism can be used for the AC systems.

Soft magnetic materials include electrical steels and soft ferrites [3, 4]. Unlike the ferromagnetic metals which are conductors, soft ferrites have low electric conductivity, i.e., they are dielectric materials. The electrical steels have extensive applications in low-frequency systems, such as generators, motors, and transformers, while the soft ferrites are suitable for the high-frequency applications, such as circulators, isolators, phase shifters, and high-speed switches.

This chapter will focus on the properties of the soft ferrites and their applications at high-frequency systems. The ferrites are crystals having small electric conductivity compared to ferromagnetic materials. Thus they are useful in high-frequency devices because of the absence of significant eddy current losses. Ferrites

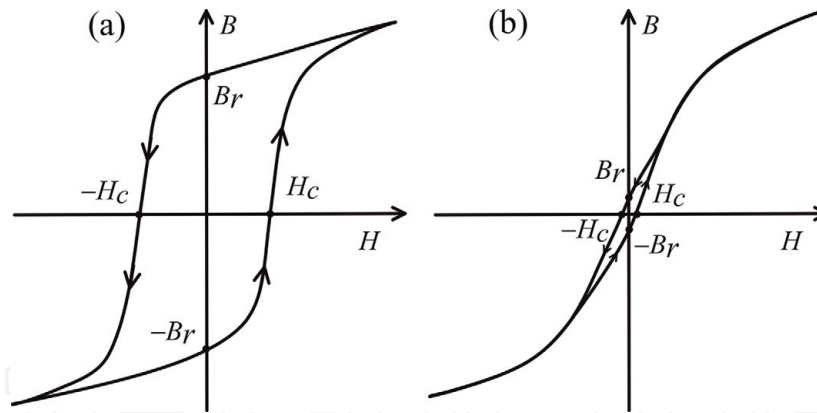


**Figure 1.**

The hysteresis (B-H) curves for (a) hard ferrimagnetism and (b) soft ferrimagnetism. The remnant polarization ( $B_r$ ) and the coercive field ( $H_c$ ) for the hard ferrites should be as large as possible. On the other hand, for the soft ferrites, the remnant polarization ( $B_r$ ) and the coercive field ( $H_c$ ) are very small or even close to zero.

are ceramic-like materials with specific resistivities that may be as much as  $10^{14}$  greater than that of metals and with dielectric constants around 10 to 16 or greater. Ferrites are made by sintering a mixture of metal oxides and have the general chemical composition  $MO \cdot Fe_2O_3$ , where M is a divalent metal such as Mn, Mg, Fe, Zn, Ni, Cd, etc. Relative permeabilities of several thousands are common [5, 6]. The magnetic properties of ferrites arise mainly from the magnetic dipole moment associated with the electron spin [2].

The magnetic dipole moment precesses around the applied DC magnetic field by treating the spinning electron as a gyroscopic top, which is a classical picture of the magnetization process. This picture also explains the anisotropic magnetic properties of ferrites, where the permeability of the ferrite is not a single scalar quantity, but instead is a generally a second-rank tensor or can be represented as a matrix. The left and right circularly polarized waves have different propagation constant along the direction of the external magnetic field, resulting in the nonreciprocity of a propagating wave. Since the permeability should be treated as a tensor (matrix), not a scalar permeability, it is generally much difficult to understand and to have intuition, even for the researchers.

## 2. The susceptibility matrix

### 2.1 Magnetic dipole precesses around the applied magnetic field

The properties of ferrites are very intriguing. Without a DC bias magnetic field  $H_0$ , the magnetic dipoles of ferrites are randomly orientated. They exhibit dielectric properties only. The dielectric loss can be high or low depending on the loss tangent of the soft ferrites. Interestingly, when the DC bias magnetic field is strong enough, and the ferrite is magnetically saturated, the magnetic dipole will precess around the DC bias field at a frequency called the Larmor frequency ( $\omega_0 \propto H_0$ ). Waves with different circular polarizations will corotate or counter-rotate with the precession of the magnetic dipoles.

**Figure 2** shows the Larmor precession with the circularly polarized fields [7]. Circular polarization may be referred to as right handed or left handed, depending on the direction in which the electric (magnetic) field vector rotates. For a

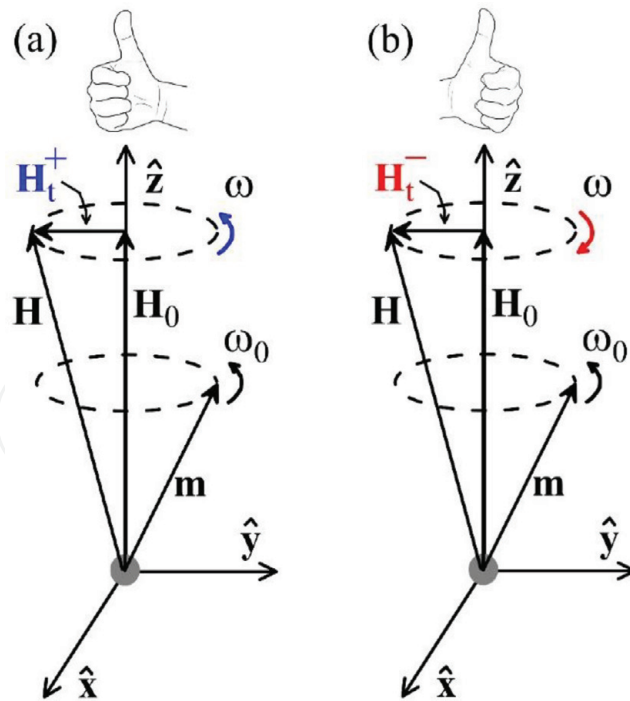


**Figure 2.** Larmor precession of a magnetic moment  $\mathbf{m}$  around the applied DC bias field  $\mathbf{H}_0 (= H_0 \hat{\mathbf{z}})$  with (a) a right-hand circularly polarized (RHCP) wave and (b) a left-hand circularly polarized (LHCP) wave. The frequency of the Larmor precession in both cases are the same, i.e., the Larmor frequency  $\omega_0 (= \mu_0 \gamma H_0)$ .  $H_t^+$  and  $H_t^-$  are the transverse components of the incident waves which rotate clockwise (RHCP) and counter-clockwise (LHCP) from the source viewpoint looking in the direction of propagation. The thumb points the direction of the wave propagation, and the fingers give the rotation of the transverse components [7].

right-hand circularly polarized (RHCP) wave, the fields rotate clockwise at a given position from the source looking in the direction of propagation. The magnetic dipole moment  $\mathbf{m}$  processes around the  $\mathbf{H}_0$  field vector, like a top spinning precess around the  $z$ -axis at the Larmor frequency  $\omega_0$ . The spinning property depends on the applied DC bias magnetic field. **Figures 2(a)** and **(b)** shows the RHCP and LHCP waves with the gyrating frequency of  $\omega$ . When the RHCP wave is propagating along the direction of the DC bias field, it corotates with the precession of the magnetic dipole moments. On the other hand, the left-hand circularly polarized (LHCP) wave will counter-rotate with the precession of the dipole moments.

A linearly polarized incident wave can be decomposed into RHCP and LHCP waves of equal amplitude. The orientation of the linearly polarized wave changes after the wave propagates a certain distance because of the distinct propagation constants. The phenomenon is the famous Faraday's rotation [5, 6]. This unique property has various applications, such as phase shifters, isolators, and circulators. However, it is difficult to follow for students and even researchers in that the permeability is a tensor, not just a simple proportional constant.

Here we consider the simplest case for the pedagogic purpose—a circularly polarized plane wave is normally incident upon a semi-infinite medium. The wave characteristics such as the propagation constant  $k$  and the wave impedance  $Z$  are associated with the permeability  $\mu$ , which is a tensor for the ferrite medium [5]. By finding the preferred eigenvalues, it will be shown that the properties of  $\mu$  depend on the DC bias field  $H_0$ , the saturated magnetization  $M_s$ , and the operating frequency  $\omega$ . By adjusting the frequency of the incident wave, i.e.,  $\omega$ , the permeability  $\mu$  changes, especially close to the Larmor frequency ( $\omega_0$ ). Such an effect is called the ferrite magnetic resonance (FMR) or gyromagnetic resonance [7].

## 2.2 Derivation of the susceptibility matrix

The permeability  $\mu_r(\omega)$  is a tensor. Note that the permittivity  $\epsilon_r(\omega)$  can be expressed in a tensor as well, but in the region of interest around 10 GHz, it can be treated as a complex proportional constant for many ceramics. Many microwave textbooks and literature have elaborated the derivation of the permeability tensor [5–7]. In this paper, a more accessible interpretation of the permeability tensor is provided. The magnetic properties of a material are due to the existence of magnetic dipole moment  $\mathbf{m}$ , which arise primarily from its (spin) angular momentum  $\mathbf{s}$ . The magnetic dipole moment and angular momentum have a simple relation,  $\mathbf{m} = -\gamma\mathbf{s}$ , where  $\gamma$  is the gyromagnetic ratio ( $\gamma = e/m = 1.759 \times 10^{11}$  C/kg). When a DC bias magnetic field  $\mathbf{B}_0 (= \mu_0\mathbf{H}_0)$  is present, the torque  $\boldsymbol{\tau}$  exerted on the magnetic dipole moment is

$$\boldsymbol{\tau} = \mathbf{m} \times \mathbf{B}_0 = \mu_0\mathbf{m} \times \mathbf{H}_0. \quad (1)$$

Since the torque is equal to the time change rate of the angular momentum, we have

$$\boldsymbol{\tau} = \frac{d\mathbf{s}}{dt} = \frac{-1}{\gamma} \frac{d\mathbf{m}}{dt}. \quad (2)$$

By comparing Eqs. (1) and (2), we obtain

$$\frac{d\mathbf{m}}{dt} = -\mu_0\gamma\mathbf{m} \times \mathbf{H}_0. \quad (3)$$

A large number of the magnetic dipole moment  $\mathbf{m}$  per unit volume give rise to an average macroscopic magnetic dipole moment density  $\mathbf{M}$ . The torque exerting on the magnetization per unit volume  $\mathbf{M}$  due to the magnetic flux  $\mathbf{H}$  has the same form as Eq. (3):

$$\frac{d\mathbf{M}}{dt} = -\mu_0\gamma\mathbf{M} \times \mathbf{H}. \quad (4)$$

$\mathbf{M}$  and  $\mathbf{H}$  in Eq. (4) differ slightly from  $\mathbf{m}$  and  $\mathbf{H}_0$  in Eq. (3) in that  $\mathbf{M}$  and  $\mathbf{H}$  can further be divided into two parts: the DC term and the high-frequency AC term. The DC term is, in general, much larger than the AC term. The applied DC bias magnetic field  $H_0$  is assumed to be in the z-direction. When  $H_0$  is strong enough, the magnetization will be saturated, denoted as  $M_s$  which aligns with the direction of  $H_0$ . If the AC term just polarizes in the transverse direction (i.e., the xy plane), the external magnetic bias field and the magnetization can be written as,

$$\mathbf{H} = H_x\hat{\mathbf{x}} + H_y\hat{\mathbf{y}} + H_0\hat{\mathbf{z}}, \quad (5)$$

$$\mathbf{M} = M_x\hat{\mathbf{x}} + M_y\hat{\mathbf{y}} + M_s\hat{\mathbf{z}}. \quad (6)$$

Since the AC terms have an  $\exp(-i\omega t)$  dependence, by substituting Eq. (5) and (6) into Eq. (4) the transverse component terms read

$$(\omega_0^2 - \omega^2)M_x = \omega_0\omega_m H_x + j\omega\omega_m H_y; \quad (7)$$

$$(\omega_0^2 - \omega^2)M_y = -j\omega\omega_m H_x + \omega_0\omega_m H_y, \quad (8)$$

where  $\omega_0 = \mu_0\gamma H_0$  and  $\omega_m = \mu_0\gamma M_s$ . In matrix representation, Eq. (7) and (8) can be rewritten as



$$\mathbf{M} = [\chi]\mathbf{H} = \begin{bmatrix} \chi_{xx} & \chi_{xy} & 0 \\ \chi_{yx} & \chi_{yy} & 0 \\ 0 & 0 & 0 \end{bmatrix} \mathbf{H}, \quad (9)$$

where  $\chi_{xx} = \chi_{yy} = \omega_0 \omega_m / (\omega_0^2 - \omega^2)$  and  $\chi_{xy} = -\chi_{yx} = j\omega \omega_m / (\omega_0^2 - \omega^2)$ . The eigenvalues of the susceptibility matrix are

$$\chi^+ = \frac{\omega_m}{\omega_0 - \omega}, \quad (10)$$

$$\chi^- = \frac{\omega_m}{\omega_0 + \omega}. \quad (11)$$

The eigenvectors corresponding to these two eigenvalues are the right-hand circularly polarized wave (RHCP, denoted as +) and the left-hand circularly polarized wave (LHCP, denoted as -), respectively. The symbols, + and -, represent positive helicity and negative helicity, respectively. The LHCP wave has a relatively mild response over the entire frequency range. On the contrary, the RHCP wave has a much more dramatic response.

The permeabilities of the RHCP and LHCP waves are

$$\mu^+ = \mu_0 \left( 1 + \frac{\omega_m}{\omega_0 - \omega} \right), \quad (12)$$

$$\mu^- = \mu_0 \left( 1 + \frac{\omega_m}{\omega_0 + \omega} \right). \quad (13)$$

Eq. (12) has a singularity when the wave frequency  $\omega$  is equal to the Larmor frequency  $\omega_0$ . This phenomenon is called the ferri-magnetic resonance (FMR, or called gyromagnetic resonance) [6]. On the contrary, Eq. (13) is relatively mild. Therefore, this study will mainly focus on the RHCP wave.

For a resonant cavity with a quality factor ( $Q$ ), the loss effect can be introduced by using the complex resonant frequency  $\omega_0(1 - i/2Q)$ . By analogy with the resonant cavity, the loss part can be calculated by using the complex frequency  $\omega_0 \rightarrow \omega_0(1 - i\Delta H\mu_0\gamma/2\omega_0)$ , where  $\Delta H$  is the ferrimagnetic resonance linewidth [2, 3]. Since

$$\frac{\Delta H\mu_0\gamma}{2\omega_0} = \frac{\Delta H\mu_0\gamma}{2H_0\mu_0\gamma} = \frac{\Delta H}{2H_0}, \quad (14)$$

the permeability for the RHCP wave now reads

$$\mu_r^+ = \left( 1 + \frac{\frac{\omega_m}{\omega_0}}{\left( 1 - \frac{\omega}{\omega_0} \right) + i \frac{\Delta H}{2H_0}} \right). \quad (15)$$

To conduct a complete simulation of a ferrite device, we need to know its complex permittivity, the saturation magnetization, and the resonance linewidth. We will discuss how to characterize the ferrite's properties in the next section.

### 3. Characterization of ferrite materials

Here we will discuss the measurement of the most important properties of ferrites, including the dielectric properties ( $\epsilon_r + i\epsilon_i$ ), the saturation magnetization

( $M_s$  or  $4\pi M_s$ ), and the resonance linewidth ( $\Delta H$ ). The behavior of the spin wave linewidth should be considered when the field strength of an electromagnetic wave exceeds a threshold value, that is, the high-power condition. For the general purpose, only the first three properties will be used in the ferrite simulation.

### 3.1 Dielectric properties

Ferrites are ceramic-like materials with relative dielectric constants around 10 to 16 or greater. The resistivities of ferrites may be as high as  $10^{14}$  greater than that of metals. Since ferrites are dielectric materials. The dielectric properties ( $\epsilon_r + i\epsilon_i$ ) always play an important role with or without the influence of the magnetic field. The perturbation method is the most commonly employed resonant technique [8, 9]. The perturbation method is very good for small-size and low-dielectric samples. When measuring the high-dielectric samples, however, the fields and the resonant frequency change drastically. The perturbation technique may lead to a reduced accuracy. Recently, the field enhancement method was proposed [10, 11]. The field enhancement method operates at a condition opposite to the perturbation method. The resonant frequency and quality factor alter significantly and depend on not only the geometry of the cavity but the sample's size and complex permittivity as well. Luckily, both the perturbation method and the field enhancement method agree well for samples with the dielectric constant below 50, which is suitable for most of the ferrites.

**Figure 3** shows the ideal of the field enhancement method. **Figure 3(a)** shows the resonant frequency as functions of the dielectric constant ( $\epsilon_r$ ) using a simulation setup as in **Figure 3(b)**. The ingot-shaped sample has a diameter of 16.00 mm and thickness of 5.00 mm. The solid blue line depicts the simulation result for the field enhancement method. From the measured resonant frequency, we can derive the corresponding dielectric constant. On the other hand, the dashed black line is obtained using a sample with the same diameter but much thinner in thickness of 1.0 mm. The response of the 1-mm-thick sample quite resembles the perturbation method. The imaginary part of the permittivity ( $\epsilon_i$ ) or the loss tangent ( $\tan \delta = \epsilon_i/\epsilon_r$ ) can then be determined from the measured resonant frequency and the quality factor. The field enhancement method has very wide measuring range from unity to high- $\kappa$  dielectrics and from lossless to lossy materials [10, 11].

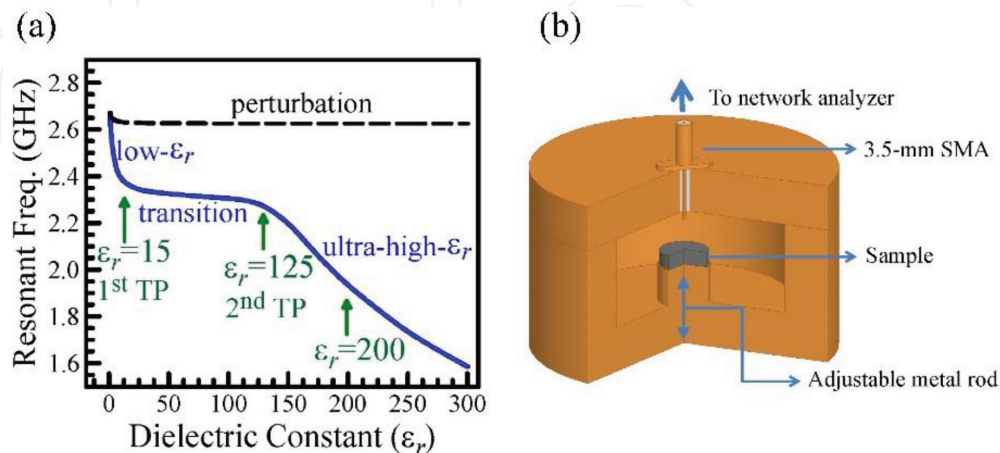


**Figure 3.**

(a) Resonant frequency versus dielectric constant based on full-wave simulations. The solid curve can be divided into three regions: low, transition, and ultrahigh. The dashed line is simulated with a much thinner sample of 1.00 mm in thickness, which exhibits the properties similar to those of perturbation. (b) Schematic diagram of the field enhancement method. It consists of a cylindrical resonant cavity and a metal rod. The sample is placed on the top of the metal rod. The metal rod focuses and enhances the electric field significantly. An SubMiniature version A (SMA) 3.5-mm adapter couples the wave from the top of the cavity [11].

### 3.2 Saturation magnetization

Ferrites have a strong response to the applied magnetic field. The magnetic properties of ferrites arise mainly from the magnetic dipole moment associated with the electron spin. Relative permeabilities of several thousands are common. The saturation magnetization ( $M_s$  or  $4\pi M_s$ ) of a ferrite plays a key role as shown in Section 2. Researchers or engineers use the saturation magnetization as a design parameter that enters into the initial selection of a ferrimagnetic material for microwave device applications. Typical ferrimagnets exhibit values of  $4\pi M_s$  between 300 gauss (G) and 5000 G. Static or low-frequency methods are generally used to measure  $4\pi M_s$  [12]. From the measured hysteresis loop as shown in **Figure 4**, one can determine the saturation magnetization  $M_s$ .

Note that the saturation magnetization is denoted as  $M_s$  in the SI unit, but since the values are generally displayed in Gaussian unit (gauss, G),  $4\pi M_s$  is commonly used. Also, the internal bias  $H_0$  is different from the applied  $H$ -field ( $H_a$ ). Demagnetization factor should be considered [5, 6]. The demagnetization factor allows us to calculate the  $H$ -field inside the sample denoted as  $H_0$ . In all, measurement of the saturation magnetization from the dynamic hysteresis loop characteristics can be used for the design and simulation of ferrite devices.

### 3.3 Resonance linewidth

The loss of ferrite material is related to the linewidth,  $\Delta H$ , of the susceptibility curve near resonance. Consider the imaginary part of the susceptibility  $\chi''_{xx}$  versus the bias field  $H_0$ . The linewidth  $\Delta H$  is defined as the width of the curve of  $\chi''_{xx}$  versus  $H_0$ , where  $\chi''_{xx}$  has decreased to half of its peak value. For a fixed microwave frequency  $\omega$ , resonance occurs when  $\omega_0 = \mu_0 \gamma H_r$ , such that  $\omega = \omega_0 (= \mu_0 \gamma H_r)$ . The linewidth,  $\Delta H$ , is defined as the width of the curve of  $\chi''_{xx}$  versus  $H_0$ , where  $\chi''_{xx}$  has decreased to half its peak value. This is the idea that is introduced in [5]. However, obtaining the relation of  $\chi''_{xx}$  versus  $H_0$  is not easy. Here we adopt another commonly used technique [9, 12].

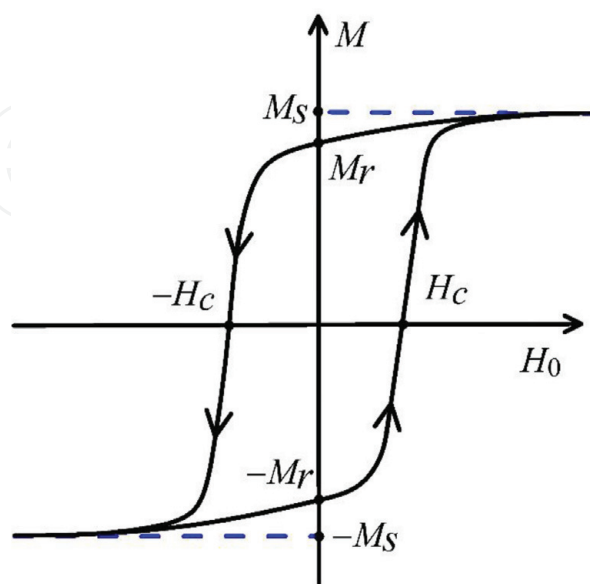


**Figure 4.** The hysteresis curve regarding the magnetization  $M$  and the internal bias  $H_0$ . When the applied internal magnetic field  $H_0$  is large enough, the magnetization will be saturated, denoted as ( $M_s$  or  $4\pi M_s$ ). When  $H_0$  decreases to zero, the remnant polarization is denoted as  $M_r$ . The polarization will change sign (from positive to negative) when  $H_0$  is greater than  $-H_c$  which is called the coercive field.



The idea is normally implemented using a  $TE_{10n}$  ( $n$  even) cavity in the X-band region [9, 12]. The test sample is placed at the  $H$ -field maximum. The sample is spherical with a diameter of approximately 0.040 inches, which is much easier to estimate than the internal bias field  $H_0$ . A cross-guide coupler is used with the coupling iris. The loaded  $Q$  ( $Q_L$ ) of the empty cavity should be 2000 or greater. The sample, mounted on a fused silica or equivalent rod, is positioned away from the cavity wall at a point of minimum microwave electric field and maximum microwave magnetic field. A power meter can be used to read off the half-power points by adjusting the DC magnetic field and measuring the difference in  $H_0$ -field directly [12]. **Figure 5** shows how the resonant linewidth is determined.

The three key parameters are obtained in three experimental setups under different sizes and geometries of the samples. If the samples' properties are slightly different or the machining error is not negligible, the error will be large or even unacceptable. The ultimate goal is to integrate the measurements and to extract the parameters using one experimental setup. The three key parameters will be used in the design of the microwave ferrite devices in the next session.

## 4. Applications of ferrite materials

The ferrites are crystals having small electric conductivity compared to ferromagnetic materials. Thus they are useful in high-frequency situations because of the absence of significant eddy current losses. Three commonly used ferrite devices are discussed below. These are phase shifters, circulators, and isolators [13–16].

### 4.1 Phase shifter

The phase shifters are important applications of ferrite materials, which are two-port components that provide variable phase shift by changing the bias magnetic field. Phase shifters find application in test and measurement systems, but the most significant use is in phase array antenna where the antenna beam can be steered in space by electronically controlled phase shifters. Because of the demand, many different types of phase shifters have been provided. One of the most useful designs is the latching nonreciprocal phase shifter using a ferrite toroid in the rectangular waveguide. We can analyze this geometry with a reasonable degree of approximation using the double ferrite slab geometry.

**Figure 6** shows the full-wave simulation for a two-port phase shifter using high-frequency structure simulator (HFSS, ANSYS). A standard waveguide WR-90 is employed with a width of 22.86 mm and height of 10.16 mm. The field patterns are

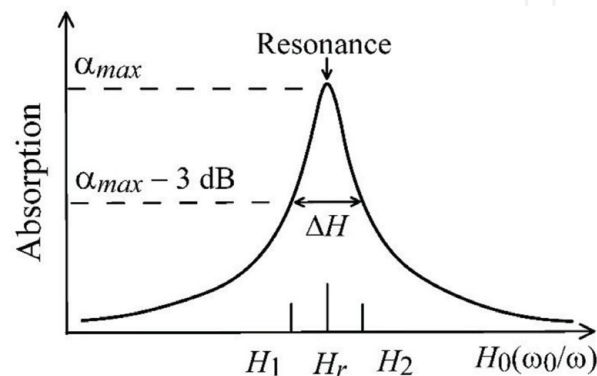


**Figure 5.**

The idea is to place the sample at the maximum of the  $H$ -field. It exhibits resonant absorption when the internal bias field is changed to  $H_r$ . By changing the magnetic field, we will obtain the absorption.  $H_1$  and  $H_2$  are associated with the 3-dB absorption. The difference between these two values is the resonance linewidth  $\Delta H$ .

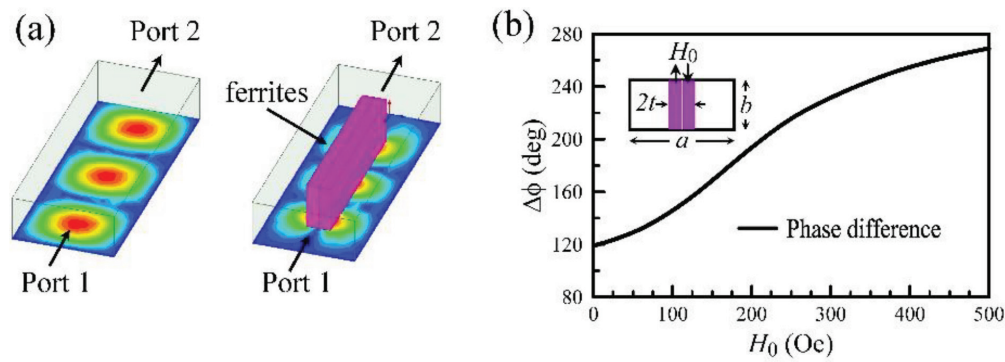


**Figure 6.** Simulation results. (a) The field pattern to the left is for the empty waveguide. The right figure shows field strength with ferrites. (b) The phase difference  $\Delta\phi$  as a function of the internal bias field  $H_0$ .

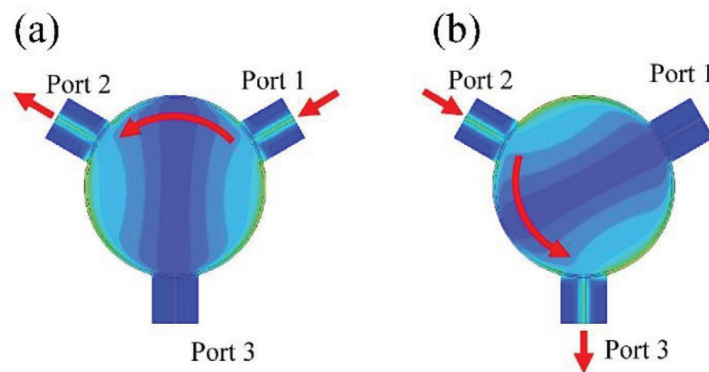


**Figure 7.** Schematic diagrams of the operation of a stripline circulator. (a) The incident wave is injected from Port 1 and the transmitted wave ideally goes to Port 2. (b) The incident wave from Port 2 will go to Port 3. The color spectrum is the electric field pattern inside the ferrite disks. It is a three-port, nonreciprocal device. A full-wave solver, high-frequency structure simulator (HFSS), is used [18].

displayed in **Figure 6(a)** for an empty waveguide and a waveguide with two ferrite slabs. The phase difference  $\Delta\phi$ , shown in **Figure 6(b)**, is calculated under two conditions: with and without ferrites. The simulation parameters are the same as example 9.4 of Pozar's textbook. The saturation magnetization ( $4\pi M_s$ ) is 1786 G, the dielectric constant  $\epsilon'$  is 13.0, and the resonance linewidth  $\Delta H$  is 20 Oe. The length and thickness of the ferrite are  $L = 37.50$  mm and  $t = 2.74$  mm.

## 4.2 Circulator

Circulator, a nonreciprocal device, has been widely used in various microwave systems. **Figure 7** schematically shows the function of a stripline circulator. The circulator is, in general, a three-port device. If the incident wave is injected from Port 1, then the wave will ideally go to Port 2, while Port 3 will be isolated as shown in **Figure 7(a)**. On the other hand, if the wave is injected from Port 2, it will go to Port 3 and isolate from Port 1 as shown in **Figure 7(b)**. There are three figures of merit for a circulator: transmission, reflection, and isolation. The transmission from Port 1 to Port 2 should be as high as possible, i.e., the insertion loss should be as small as possible. The reflection received at Port 1 due to the incident wave of Port 1 ( $S_{11}$ ) and the isolation from Port 1 to Port 3 ( $S_{13}$ ) should be as small as possible. The nonreciprocity of the circulator can be used to protect the oscillators from the damage of the reflected power in plasma or material processing systems. It can also be used to separate the transmitted and the received waves in radar or communication systems [13–17].

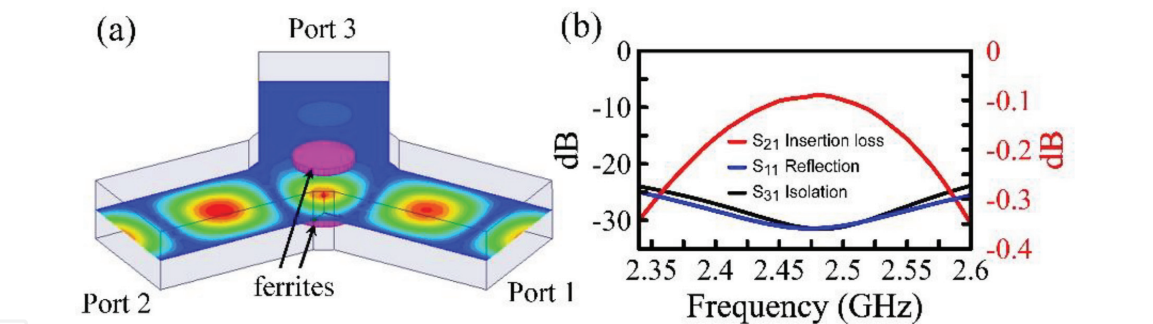


**Figure 8.** (a) Schematic diagrams of the operation of a waveguide circulator. A full-wave solver, HFSS, is used with the saturation magnetization ( $4\pi M_s$ ) is 1600 G, the dielectric constant  $\epsilon'$  is 13.0, and the resonance linewidth  $\Delta H$  is 10 Oe. The radius and thickness of the ferrite disks in rust red are  $R = 21.0$  mm and  $t = 5$  mm, respectively. The waveguide is a standard WR 340 with  $86.36 \times 43.18$  mm<sup>2</sup>. The electric field pattern is displayed in color. (b) Simulation results of the waveguide circulator like the one in Part (a). The solid red curve is the transmission or insertion loss; the blue curve represents the reflection loss, and the black is the isolation.

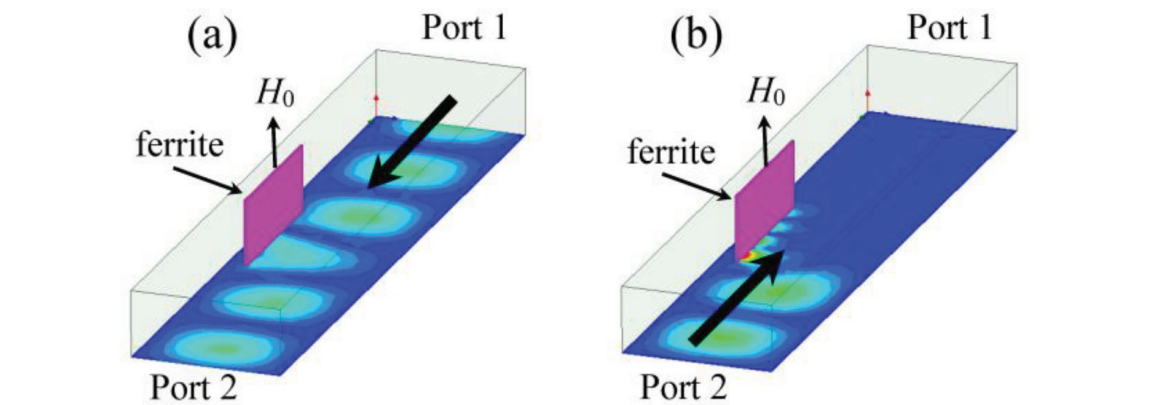


**Figure 9.** The simulated field strength for a two-port isolator using the full-wave solver. (a) The high forward transmission ( $S_{21}$ ) and (b) the low reverse transmission ( $S_{12}$ ). The saturation magnetization ( $4\pi M_s$ ) is 1700 G, the dielectric constant  $\epsilon'$  is 13.0, and the resonance linewidth  $\Delta H$  is 200 Oe. The length and thickness of the ferrite are  $L = 24.0$  mm and  $t = 0.5$  mm.

In addition to the stripline circulator, there are other types such as the microstrip circulator and the waveguide circulator. The microstrip circulator is similar to the stripline circulator in many ways. Here we show a waveguide circulator which is capable of high-power operation. **Figure 8(a)** shows the structure of the nonreciprocal device and the simulated electric field strength. The simulation parameters are described in the caption. The circulator is, in general, a three-port device. If the incident wave is injected from Port 1, then the wave will ideally go to Port 2, while Port 3 will be isolated as shown in **Figure 8(b)**. On the other hand, if the wave is injected from Port 2, it will go to Port 3 and be isolated from Port 1 as shown in **Figure 8(b)**.

### 4.3 Isolator

The isolator is one of the useful microwave ferrite components. As shown in **Figure 9**, the isolator is generally a two-port device having unidirectional transmission characteristics (nonreciprocity). From Port 1 to Port 2 ( $S_{21}$ ), the forward transmission is high (i.e., low insertion loss in **Figure 9(a)**). However, from Port 2 to Port 1 ( $S_{12}$ ), the reverse transmission is low (i.e., high isolation in **Figure 9(b)**). Besides, the reflection ( $S_{11}$  and  $S_{22}$ ) should be as low as possible. The simulation parameters in **Figure 9** are the same as Ex. 9.2 of Pozar's textbook [5]. The simulation parameters and the sample's geometry are described in the caption.

An isolator is commonly used to prevent the high reflected power from damaging the precious and expansive microwave source. For example, the impedance of a plasma system changes a lot when the plasma is ignited. The radical change of the impedance will result in impedance mismatch and cause serious reflection which might kill the source instantly. An isolator can be used in place of a matching or tuning network. However, it should be realized that the reflected power will be absorbed by the ferrite of the isolator, as shown in **Figure 9(b)**. When the ferrite absorbs the reflected energy, the temperature will rise and the performance will be compromised. Therefore, a simple isolator can be implemented by using a circulator with one port well terminated [19]. For example, if Port 3 in **Figure 8(a)** is matched with water load, the power injected from Port 2 will go to Port 3 and will be isolated from Port 1. The power handling capability can be improved.

Circulator and isolator can be implemented using the self-bias [20–22], just like the latch phase shifter ( $H_0 = 0$ ) shown in **Figure 6** using the remnant field  $B_r$  or  $M_r$  only. The self-biased ferrite devices will simplify the design and fabrication, but the overall performance is still not good enough. Further theoretical and experimental study is needed.

## 5. Conclusions

Ferrimagnetism and ferromagnetism share many magnetic properties in common, such as hard and soft magnets, but the conductivity differentiates these two materials. Ferrites are ceramic materials and suitable for the high-frequency operation. The electromagnetic properties of ferrite materials are difficult to understand in that the magnetic susceptibility is a tensor and depends on the saturated magnetization  $M_s$ , the internal bias field  $H_0$ , and the resonance linewidth  $\Delta H$ . The magnetic susceptibility also depends on the frequency of the microwave  $\omega$  as well as the polarization of the wave. The first two sessions explain the basic properties.

The complex permittivity  $\epsilon_r + i\epsilon_i$ , the saturation magnetization  $M_s$ , and the resonance linewidth  $\Delta H$  are the most important electromagnetic properties of ferrites. How to measure the ferrite's properties are discussed in Section 3. The full-wave simulation is conducted to demonstrate how the phase shifter, circulator, and isolator work, which are shown in Section 4. Although the examples are discussed in many textbooks, Section 4 offers in-depth simulation results for the first time.

At high-power operation, the ferrite devices will be heated. The spin wave linewidth may be taken into account. Besides, the ferrites will become paramagnetism when the temperature exceeded the Curie temperature. These two factors are important for high-power operation, which are not considered in this chapter.

## Acknowledgements

This chapter was supported in part by the Ministry of Science and Technology of Taiwan and in part by China Steel Company/HIMAG Magnetic Corporation, Taiwan. The author is grateful to the Taiwan Branch of ANSYS Inc. for technical assistance and to Dr. Hsein-Wen Chao and Mr. Wei-Chien Kao for their assistance in the full-wave simulation. Dr. Hsin-Yu Yao and Mr. Shih-Chieh Su are appreciated for the discussion of the ferrites' characterization.



IntechOpen

IntechOpen

### **Author details**

Tsun-Hsu Chang

Department of Physics, National Tsing Hua University, Hsinchu, Taiwan

\*Address all correspondence to: [thschang@phys.nthu.edu.tw](mailto:thschang@phys.nthu.edu.tw)

### **IntechOpen**

---

© 2019 The Author(s). Licensee IntechOpen. This chapter is distributed under the terms of the Creative Commons Attribution License (<http://creativecommons.org/licenses/by/3.0>), which permits unrestricted use, distribution, and reproduction in any medium, provided the original work is properly cited. 



## References

- [1] Okamoto A. The invention of ferrites and their contribution to the miniaturization of radios. *IEEE Globecom Workshops*. 2009;1-42. DOI: 10.1109/GLOCOMW.2009.5360693. ISBN 978-1-4244-5626-0
- [2] Néel L. Magnetic Properties of Ferrites: Ferrimagnetism and Antiferromagnetism. *Annales de Physique*. 1948;3:137-198
- [3] Chen CW. Magnetism and Metallurgy of Soft Magnetic Materials. Elsevier; 1977. 15–60 p. DOI: 10.1016/B978-0-7204-0706-8.X5001-1. ISBN: 9780444601193
- [4] McGrayne SB, Suckling EE, Kashy E, Robinson FNH, Bleaney B. Magnetism Physics; 2018. Available from: <https://www.britannica.com/science/magnetism/> [Accessed: 2018-12-20]
- [5] Pozar DM. Chap. 9. In: *Microwave Engineering*. 4th ed. Hoboken, New Jersey: John Wiley & Sons, Inc.; 2011
- [6] Collin RE. Chap. 6. In: *Foundations for Microwave Engineering*. 2nd ed. New York: McGraw Hill; 1992
- [7] Chang TH. Gyromagnetically-induced transparency for ferrites. *American Journal of Physics*. 2016;84:279-283
- [8] Cohn SB, Kelly KC. Microwave measurement of high-dielectric-constant materials. *IEEE Transactions on Microwave Theory and Techniques*. 1966;14:406-410
- [9] Chen LF, Ong CK, Neo CP, Varadan VV, Varadan VK. *Microwave Electronics: Measurement and Materials Characterization*. Hoboken, New Jersey: John Wiley & Sons Inc.; 2004
- [10] Chao HW, Wong WS, Chang TH. Characterizing the complex permittivity of high- $\kappa$  dielectrics using enhanced field method. *The Review of Scientific Instruments*. 2015;86:114701
- [11] Chao HW, Chang TH. Wide-range permittivity measurement with a parametric-dependent cavity. *IEEE Transactions on Microwave Theory and Techniques*. 2018;66:4641-4648
- [12] Skyworks. Test for Line Width and Gyromagnetic Ratio [Internet]. 1999. Available from: [http://www.skyworksinc.com/uploads/documents/Test\\_for\\_Line\\_Width\\_Gyromagnetic\\_Ratio\\_202837B.pdf](http://www.skyworksinc.com/uploads/documents/Test_for_Line_Width_Gyromagnetic_Ratio_202837B.pdf) [Accessed: 2018-12-20]
- [13] Fuller AJB. *Ferrites at Microwave Frequencies*. London: Peter Peregrinus; 1987
- [14] Pardavi-Horvath M. Microwave applications of soft ferrites. *Journal of Magnetism and Magnetic Materials*. 2000;215:171-183
- [15] Schloemann E. Advances in ferrite microwave materials and devices. *Journal of Magnetism and Magnetic Materials*. 2000;209:15-20
- [16] Harris VG, Geiler A, Chen Y, Yoon SD, Wu M, Yang A, et al. Recent advances in processing and applications of microwave ferrites. *Journal of Magnetism and Magnetic Materials*. 2009;321:2035-2047
- [17] Helszajn J. *The Stripline Circulators: Theory and Practice*. Hoboken, New Jersey: John Wiley & Sons; 2008
- [18] Chao HW, Wu SY, Chang TH. Bandwidth broadening for stripline circulator. *The Review of Scientific Instruments*. 2017;88:024706
- [19] Linkhart DK. *Microwave Circulator Design*. 2nd ed. Norwood, MA: Artech House Microwave Library; 2014

[20] Wang J, Yang A, Chen Y, Chen Z, Geiler A, Gillette SM, et al. Self-biased Y-junction circulator at K<sub>u</sub>-band. *IEEE Microwave and Wireless Components Letters*. 2011;**21**:292-294

[21] Peng B, Xu H, Li H, Zhang W, Wang Zhang YW. Self-biased microstrip junction circulator based on barium ferrite thin films for monolithic microwave integrated circuits. *IEEE Transactions on Magnetics*. 2011;**47**: 1674-1677

[22] Zuo X, How H, Somu S, Vittoria C. Self-biased circulator/isolator at millimeter wavelengths using magnetically oriented polycrystalline strontium M-type hexaferrite. *IEEE Transactions on Magnetics*. 2003;**39**: 3160-3162